JPE 17-3-14

https://doi.org/10.6113/JPE.2017.17.3.716
ISSN(Print): 1598-2092 / ISSN(Online): 2093-4718

Voltage Distortion Suppression for Off-grid Inverters with an Improved Load Current Feedforward Control

Yiwen Geng[†], Xue Zhang[*], Xiaoqiang Li[**], Kai Wang[*], and Xibo Yuan[***]

[†,*]School of Electrical and Power Engineering, China University of Mining and Technology, Xuzhou, China
[**]School of Electrical and Electronic Engineering, Nanyang Technological University, Singapore
[***]Department of Electrical and Electronic Engineering, University of Bristol, Bristol, UK

Abstract

The output voltage of an off-grid inverter is influenced by load current, and the voltage harmonics especially the 5th and 7th are increased with nonlinear loads. In this paper, to attenuate the output voltage harmonics of off-grid inverters with nonlinear loads nearby, a load current feedforward is proposed. It is introduced to a voltage control loop based on the Positive and Negative Sequence Harmonic Regulator (PNSHR) compensation to modify the output impedance at selective frequencies. The parameters of the PNSHR are revised with the output impedance of the off-grid inverter, which minimizes the output impedance of the off-grid inverter. Experimental results verify the proposed method, showing that the output voltage harmonics caused by nonlinear loads can be effectively suppressed.

Key words: Load current feedforward, Output impedance, Positive and negative sequence harmonic regulator (PNSHR), Voltage harmonics

I. INTRODUCTION

With the increasing energy demand and the need to reduce the environmental impact of conventional energy sources, distributed power generation systems based on renewable energy sources, such as wind and solar energy, have become more attractive in recent years [1]-[3]. Considering that distributed renewable energy power generation is not restricted by region or grid, research on autonomous microgrids with multiple distributed generation units is in full swing [4], [5]. off-grid inverters, as the interface between power generation systems and local loads, play an important role in ensuring the high quality power injected into power systems [6], [7]. In this case, the control systems of off-grid inverters, which generally have a multi-loop structure, determine the output voltage stability [8].

Since off-grid systems are not controlled by the power grid, there are a lot of factors with regard to stability. Due to the special application of off-grid inverters in DG systems, there are several issues to be considered. An important issue is the high performance control to ensure that the converter system output voltage closely tracks the desired references with good transient and steady-state performances [9]. Nonlinear loads can affect the output voltage of an off-grid inverter, which is a difficult problem to solve [10]. In practice, the power sources in distributed generation systems may be very close to the loads, and the output current of the power sources contains a lot of low-order frequencies harmonics [11], [12]. In return, these current harmonics further distort the output voltage of the off-grid inverter [13] or even affect the stability of the overall system [14].

To improve the control performance of off-grid inverters, some progress has been made for harmonics suppression with nonlinear loads. A feedforward control strategy is often applied to suppress harmonics. Full-feedforward functions are derived in [15] and [16], which consists of three terms. These terms are the proportional term, the derivative term and the second-order derivative term. They can effectively suppress the current distortion arising from grid voltage harmonics.

Manuscript received Apr. 21, 2016; accepted Feb. 13, 2017
Recommended for publication by Associate Editor Sung-Jin Choi.
[†]Corresponding Author: gengyw556@126.com
Tel: +86-51683885667, Fax: +86-51683885667, China University of Mining and Technology
[*]School of Electrical & Power Engineering, China University of Mining and Technology, China
[**]School of Electrical and Electronic Engineering, Nanyang Technological University, Singapore
[***]Department of Electrical and Electronic Engineering, University of Bristol, UK

Thus, the steady-state error of the injected current can be substantially reduced. In [17], a full feedforward strategy is adopted to avoid non-ideal high-frequency noise. In addition, a simplified feedforward strategy is proposed to improve the dynamic performances. The analysis process ignores the delay in the current control loop, which can affect the dynamic response of the system.

As analyzed above, this paper adopts a Quasi Proportional-Resonant (Quasi-PR) voltage controller to implement load voltage compensation to reduce steady-state errors [18]. A proportional controller is designed in the inner current loop to improve the dynamic performance of the system [19]. An LC filter is installed at the output terminal of the off-grid inverter to attenuate the switching frequency harmonics [20], [21].

In order to handle the output voltage of the load variation in a dual-closed-loop control system, this paper investigates the influence of load current harmonics on the output voltage of off-grid inverters from the perspective of output impedance. It also proposes a load current feedforward compensation strategy to modify the output impedance at the selective frequency. A load current feedforward compensation strategy based on a Positive and Negative Sequence Harmonic Regulator (PNSHR) is adopted to reduce the output impedance and suppress voltage distortion. In Section II, a mathematical model of an off-grid inverter using dual-closed-loop control in the α-β frame is presented, and an output impedance model with load current feedforward is derived based on the complex transfer function. Section III studies the dual-closed-loop control strategy and the load current full feedforward strategy based on the derived output impedance model. In Section IV, a load current feedforward compensation strategy based on PNSHR is proposed, and the parameters are revised. Section V concludes the paper.

II. Output Impedance Model Based on a Complex Transfer Function

Fig. 1 shows the power circuit of a three-phase off-grid voltage source inverter (VSI) with an LC filter, where L and C_f are the inductor and capacitor, respectively, C is the DC-link capacitor, R represents the load, i_k (k=a, b, c) denotes the inverter-side currents, i_{ck} (k=a, b, c) represents the capacitor currents, and i_{ok} (k=a, b, c) is the three-phase load currents. TABLE I shows the inverter's main parameters.

According to Fig. 1, the mathematical model in the stationary a-b-c frame is derived as:

$$\begin{cases} u_{inv-abc}(t) = u_{c-abc}(t) + Lp\left[i_{abc}(t)\right] \\ \left[i_{abc}(t)\right] = \left[i_{o-abc}(t)\right] + C_f p\left[u_{c-abc}(t)\right] \end{cases} \quad (1)$$

where, $[u_{inv\text{-}abc}(t)]=[u_{inva}(t),\ u_{invb}(t),\ u_{invc}(t)]^{\mathrm{T}}$ are the output voltages of the off-grid inverter in the stationary a-b-c frame, $[u_{c\text{-}abc}(t)]=[u_{ca}(t),\ u_{cb}(t),\ u_{cc}(t)]^{\mathrm{T}}$ are the load voltages, $[i_{abc}(t)]=[i_a(t),\ i_b(t),\ i_c(t)]^{\mathrm{T}}$ are the inductor currents in the stationary a-b-c frame, and $[i_{o\text{-}abc}(t)]=[i_{oa}(t),\ i_{ob}(t),\ i_{oc}(t)]^{\mathrm{T}}$ are the load currents. The stationary a-b-c to α-β transformation used in this paper is defined as:

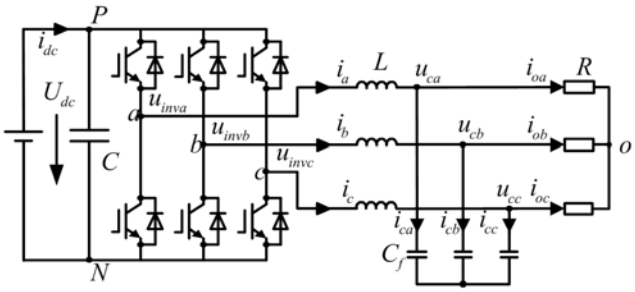

Fig. 1. Power circuit of a three-phase off-grid VSI.

TABLE I
System Parameters

Symbol	Parameter	Value
U_{dc}	DC-link voltage	650V
U_c	AC output voltage	$230V_{RMS}$
f	Fundamental frequency	50Hz
C	DC-link capacitor	2200μF
L	Filter inductor	2.7mH
C_f	Filter capacitor	20μF
f_s	Sampling frequency	5kHz

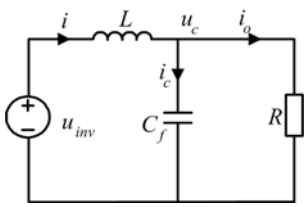

Fig. 2. Mathematical model of an LC filter.

$$x_{\alpha\beta}(t) = \left[C\right]\left[x_{abc}(t)\right], \left[C\right] = \frac{2}{3}\begin{bmatrix} 1 & -1/2 & -1/2 \\ 0 & \sqrt{3}/2 & -\sqrt{3}/2 \end{bmatrix} \quad (2)$$

where, $[x_{\alpha\beta}(t)]=[x_\alpha(t),\ x_\beta(t)]$T are stationary α-β frame time-varying quantities, $[x_{abc}(t)]=[x_a(t),\ x_b(t),\ x_c(t)]$T are stationary a-b-c frame quantities. Substituting (2) into (1), the mathematical model of the main circuit in the stationary α-β frame is obtained as:

$$\begin{cases} u_{inv-\alpha\beta}(t) = u_{c-\alpha\beta}(t) + Lp\left[i_{\alpha\beta}(t)\right] \\ \left[i_{\alpha\beta}(t)\right] = \left[i_{o-\alpha\beta}(t)\right] + C_f p\left[u_{c-\alpha\beta}(t)\right] \end{cases} \quad (3)$$

where, $[u_{inv\text{-}\alpha\beta}(t)]=[u_{inv\alpha}(t),\ u_{inv\beta}(t)]$T are the output voltages of the off-grid inverter output voltages in the stationary α-β frame, $[u_{c\text{-}\alpha\beta}(t)]=[u_{c\alpha}(t),\ u_{c\beta}(t)]$T are the voltages of the load in the stationary α-β frame, $[i_{\alpha\beta}(t)]=[i_\alpha(t),\ i_\beta(t)]$T are the inductor currents in the stationary α-β frame, $[i_{o\text{-}\alpha\beta}(t)]=[i_{o\alpha}(t),\ i_{o\beta}(t)]$T are the load currents in the stationary α-β frame, and p is the differential operator.

The mathematical model is shown in Fig. 2 [22], [23].

Fig. 3 illustrates the control scheme for an off-grid inverter with inverter-side current and output capacitor voltage

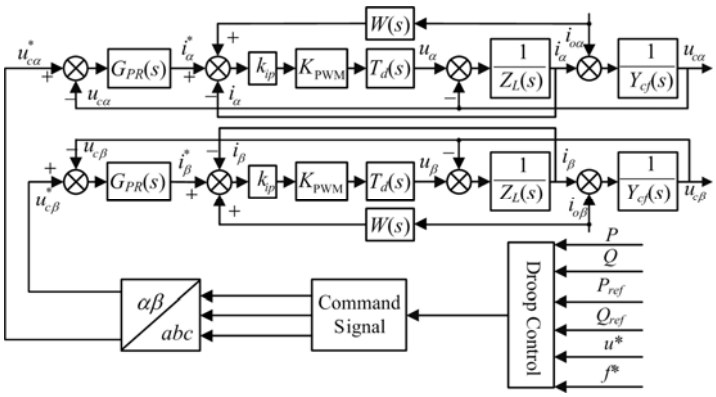

Fig. 3. Block diagram of an off-grid inverter dual-closed-loop control structure.

feedback. For different values of P and Q, the corresponding command voltage is achieved by droop control. Theoretically, Q is related to the amplitude of the voltage and P is related to the frequency. The inverter-side current is used to be parametric in the control and for over-current protection. Using capacitor voltage feedforward can improve the ability to resist disturbances of the system and to reduce the starting current. A quasi-PR voltage controller is adopted to eliminate the steady-state error. A proportional current controller improves the dynamic performance of the system. W(s) is the transfer function of the load current feedforward correction term, GPR(s) is the transfer function of the quasi-PR regulator for the voltage loop, $Z_L(s)$ is the impedance of L, $Y_{Cf}(s)$ is defined as the admittance of C_f, kip is the proportional controller for the inner current loop, and K_{PWM} is the PWM gain of the inverter. T_d(s) is the transfer function of the equivalent delay term, which is obtained by applying a first-order Pade approximation to the computation delay and the zero-order hold expression.

Thus, the digital control transfer function of T_d(s) is approximated as [24]:

$$T_d(s) \approx e^{-1.5T_s s} \approx \frac{1-0.5T_s s}{(1+0.5T_s s)^2} \tag{4}$$

where, Ts refers to the sampling period.

An off-grid inverter system contains multiple inputs and outputs in the stationary α-β frame. The complex transfer function method can greatly simplify the computation in establishing the symmetric mathematical model, which has significant advantages [25]. From Fig. 2 and Fig. 3, the transfer function of an off-grid inverter with an LC filter can be expressed as:

$$\begin{cases} Z_L(s)\boldsymbol{i} = \boldsymbol{u} - \boldsymbol{u}_c \\ Y_{cf}(s)\boldsymbol{u}_c = \boldsymbol{i}_c \\ \boldsymbol{i}_o = \boldsymbol{i} - \boldsymbol{i}_c \\ \boldsymbol{u} = \left[(u_c^* - u_c)G_{PR}(s) + \boldsymbol{i}_o W(s) - \boldsymbol{i} \right] k_{ip} K_{PWM} T_d(s) \end{cases} \tag{5}$$

where, $i=i_\alpha+ji_\beta$, $i_c=i_{c\alpha}+ji_{c\beta}$, $i_o=i_{o\alpha}+ji_{o\beta}$, $u=u_\alpha+ju_\beta$ and $u_c=u_{c\alpha}+ju_{c\beta}$ are the voltages of the load. $Y_{Cf}(s)=sC_f$ and $Z_L(s)=sL$.

According to (5), the complex transfer function of the off-grid inverter output voltage can be expressed as:

$$u_c = G_v(s)u_c^* - Z_o(s)i_o \tag{6}$$

where, $G_v(s)$ and $Z_o(s)$ are the voltage gain and output impedance of the transfer function, respectively. They are expressed in (7) and (8) as:

$$G_v(s) = \frac{G_{PR}(s)k_{ip}F_m(s)}{1+Z_L(s)Y_{cf}(s)+\left[G_{PR}(s)+Y_{cf}(s)\right]k_{ip}F_m(s)} \tag{7}$$

$$Z_o(s) = \frac{Z_L(s)+\left[1-W(s)\right]k_{ip}F_m(s)}{1+Z_L(s)Y_{cf}(s)+\left[G_{PR}(s)+Y_{cf}(s)\right]k_{ip}F_m(s)} \tag{8}$$

$$F_m(s) = K_{\mathrm{PWM}}T_d(s) \tag{9}$$

As shown in Fig.3, the transfer function of the quasi-PR regulator is as follows:

$$G_{PR}(s) = k_p + \frac{2k_i\omega_{c1}s}{s^2+2\omega_{c1}s+\omega_0^2} \tag{10}$$

III. Load Current Feedforward Scheme and Output Impedance Analysis

According to (6), the actual output voltage contains two parts, one comes from the reference output voltage with the gain $G_v(s)$ and the other comes from the load current with the output impedance $Z_o(s)$. When the load current is distorted, a lot of low-order harmonics occur in the output voltage. In this paper, the load current feedforward compensation term $W(s)$ is introduced to eliminate the influence of load current on the output voltage.

A. Load Current Unity Feedforward Scheme

According to Fig. 3, if the feedforward compensation term W(s)=1, i.e. unity feedforward control strategy, the load current is offset by the inductor current and the control strategy of the single voltage loop is adopted.

$$W(s) = 1 \tag{11}$$

Then, the output impedance can be expressed as:

$$Z_o(s) = \frac{Z_L(s)}{1+Z_L(s)Y_{cf}(s)+\left[G_{PR}(s)+Y_{cf}(s)\right]K_{\mathrm{PWM}}T_d(s)} \tag{12}$$

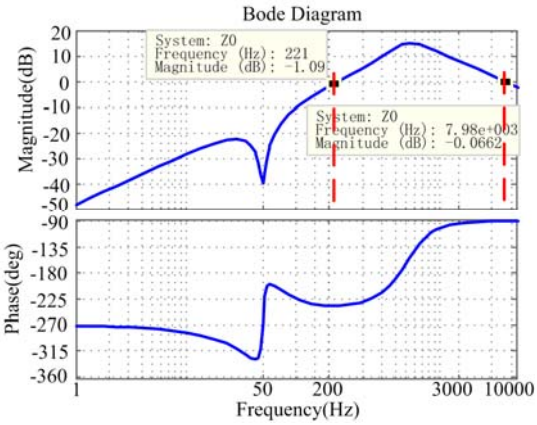

Fig. 4. Bode plots of the output impedance Zo(s).

Fig. 4 shows Bode plots of the output impedance under the single voltage loop control with the parameters shown in TABLE I. The parameters of the quasi-PR regulator are chosen as k_p=0.08, k_i=10, and w_{c1}=10rad/s. From the perspective of the output impedance, if the output impedance is approximately equal to 0, the load current disturbance for the output voltage can be ignored. It can be seen that the value of the output impedance above 0 dB is between 230Hz and 7980 Hz. In addition, the main frequency range of the harmonics is also generated by nonlinear loads. This makes the output voltage of the off-grid inverter more easily affected by load current distortions. It should be remembered that the aim is mainly the output voltage stability, and that the voltage needs to be static for load disturbance. The speed of the single voltage loop is slower than that of the dual loop [26].

B. Load Current Full-feedforward Scheme

A single voltage loop is not adequate to ensure the stability of a system. Thus, an inner loop incorporating the feedback of the inductor current is usually employed. By cascading the inner loop with the outer loop, a dual-closed-loop control strategy is constructed.

A block diagram of a dual-closed-loop control system is shown in Fig. 3. As can be seen, the load current disturbance is in the voltage loop and outside the current loop. When a load current disturbance appears, it first makes a deviation on uc, which deviates from its given value. Then the voltage loop begins to resist the disturbance and starts the adjustment process. However, the slow response of the voltage loop adjustment and the control delay of the current loop lead to a larger deviation in the dynamic process of uc.

Dual-closed-loop control achieves good control performance. However, it lacks load current control. The output voltage uc deviates from the given voltage value of u_c* with changes of the load current. As a result, the load current for the whole control system is an external disturbance signal. Theoretically, the introduction of feedforward control can overcome the shortcomings of a slower voltage adjustment and improve the dynamic response of the system, which can reduce the influence of load disturbances on the system [27].

Under ideal conditions, if the output impedance $Z_o(s)$=0, the load current disturbance can be completely eliminated, which can improve the adaptive ability of the off-grid inverter. The transfer function of the load current feedforward correction term can be derived in (13), based on (8) with $Z_o(s)$=0.

$$W(s)=\frac{sL+k_{ip}K_{\mathrm{PWM}}T_d(s)}{k_{ip}K_{\mathrm{PWM}}T_d(s)} \tag{13}$$

According to (13), neglecting the delay $T_d(s)$, $W(s)$ only contains the first-order differential term. Whether the load current feedforward is fully implemented depends on the accuracy of the filter parameters. However, the inductance parameters have a certain deviation, which has an effect on the feedforward control. Further, the introduction of the time delay term makes the feedforward control more complex.

IV. Harmonics Compensation Strategy with Load Current Feedforward

A. Load Current Feedforward Compensation Based on a PNSHR Regulator

The output current harmonics caused by the background harmonics of a power grid are suppressed by designing the output impedance in [23]. Off-grid inverters are studied to suppress the output voltage harmonics caused by nonlinear loads. Instead of grid voltage feedforward, load current feedforward is used. Normally, nonlinear loads generate odd harmonics such as the 5th, 7th, 11th and 13th. It is unnecessary to compensate load current in the whole frequency range. This paper aims to suppress the load current harmonics in view of the positive and negative sequence harmonics, and it proposes a harmonic compensation strategy based on a feedforward control with a PNSHR. In terms of the positive sequence load current harmonic component, the regulator transfer function can be expressed as:

$$G_P(s)=\frac{A\omega_c}{s-j\omega_{0h}+\omega_c} \tag{14}$$

The negative sequence harmonic regulator transfer function can be given by:

$$G_N(s)=\frac{A\omega_c}{s+j\omega_{0h}+\omega_c} \tag{15}$$

where A is the gain of the regulator, ω_{0h} is the angular frequency of the odd harmonics, and ω_c is the cutoff frequency. In consideration of system stability, ω_c=10rad/s is adopted.

Normally, the 5th and 11th harmonics are negative sequence, while the 7th and 13th are the positive sequence. The transfer function of the load current feedforward correction term for the 5th, 7th, 11th and 13th harmonics can be expressed as:

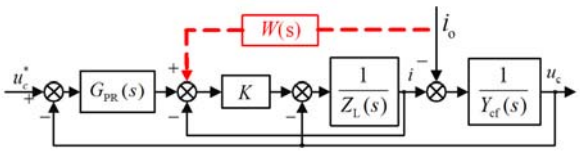

Fig. 5. Load current feedforward control strategy with a PNSHR regulator.

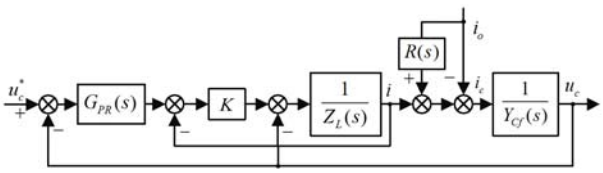

Fig. 6. Equivalent load current feedforward control strategy of Fig. 5.

$$W(s) = G_{N5}(s) + G_{P7}(s) + G_{N11}(s) + G_{P13}(s) \tag{16}$$

The load current feedforward control strategy with a PNSHR regulator for off-grid inverters is shown in Fig. 5.

B. Parameter Correction of a PNSHR Regulator

As shown in Fig. 5, the load current feedforward control strategy feeds forward the load current feedforward correction term W(s), which contains both positive and negative sequence current. Assume that s=-jω5, then G(-jω5)=A. Similarly, assume that s=jω7, then G(jω7)=A. Generally, a controller gain of A=1 cannot effectively compensate the harmonic current. Thus, the PNSHR regulator parameters need to be modified to improve the harmonic compensation performance. An equivalent voltage control scheme can be obtained by moving the load current feedforward term of Fig. 5 to the ic node, as shown in Fig. 6. R(s) can be given by:

$$R(s) = \frac{KW(s)}{sL + K} \tag{17}$$

where, K=$k_{ip}K_{PWM}T_d(s)$. If R(jω_{0h})=1, the positive and negative sequence harmonics injected from the load current can be completely compensated.

According to (17), define F(s) as:

$$F(s) = \frac{K}{sL + K} = \frac{k_{ip}\dfrac{1 - 0.5T_s s}{(1+0.5T_s s)^2}}{sL + k_{ip}\dfrac{1 - 0.5T_s s}{(1+0.5T_s s)^2}} \tag{18}$$

Then, R(s) can be rewritten as:

$$R(s) = W(s)F(s) \tag{19}$$

According to the above analysis, in order to realize full compensation of the load current harmonics, the feedforward correction term at the frequency ωh should be satisfied as:

$$\begin{cases} \| W(j\omega_h) \| = \dfrac{1}{\| F(j\omega_h) \|} \\ \angle W(j\omega_h) + \angle F(j\omega_h) = 2k\pi, (k = 0, 1, 2 \cdots\cdots) \end{cases} \tag{20}$$

TABLE II
PARAMETERS OF THE POSITIVE AND NEGATIVE SEQUENCE HARMONICS REGULATOR

Parameter	Original Value	Revised Value
A_{N5}	1	1.0609
ω_{N05}	1570	1564.5
A_{P7}	1	1.2183
ω_{P07}	2198	2210.3

Through a further derivation, found in the appendix, the revised PNSHR is obtained and the revised positive-sequence can be expressed as:

$$\begin{cases} A_h = \dfrac{\sqrt{1 + \tan \angle F(j\omega_h)^2}}{\| F(j\omega_h) \|} \\ \omega_{0h} = \omega_h - \omega_c \tan \angle F(j\omega_h) \end{cases} \tag{21}$$

The revised expression of the negative-sequence is described as:

$$\begin{cases} A_h = \dfrac{\sqrt{1 + \tan \angle F(j\omega_h)^2}}{\| F(j\omega_h) \|} \\ \omega_{0h} = \omega_h + \omega_c \tan \angle F(j\omega_h) \end{cases} \tag{22}$$

To verify the proposed strategy, the off-grid inverter output impedance before and after the revision of the PNSHR regulator parameters are analyzed with the 5th and 7th load current harmonics considered. Both positive and negative sequence controllers are adopted in the proposed method. According to the system parameters shown in Table I, the positive and negative sequence harmonic regulator parameters can be modified according to (21) and (22), as shown in Table II.

Fig. 7 shows the magnitude-frequency characteristics of the output impedance with the following three strategies. Curve I shows a control strategy with the unity feedforward control strategy. Curve II represents the feedforward control strategy without a PNSHR. Curve III indicates the feedforward control strategy with PNSHR parameters revision.

Fig. 7(a) shows the magnitude-frequency characteristics of the 5th negative-sequence harmonic, while Fig. 7(b) shows that of the 7th positive-sequence harmonic. By comparison, the control strategy with the unity feedforward control strategy shows that the output impedance magnitude can be attenuated in the low-frequency range and does not reduce at the 7th harmonic frequency. Compared with the feedforward control strategy without PNSHR parameters revision, the amplitude reduction is quite small, and the frequencies contains deviations where the impedance magnitude is attenuated, which affects the performance of the harmonic suppression. When the feedforward control strategy with PNSHR parameters revision is adopted, the impedance magnitude is attenuated more effectively at the 5th and 7th

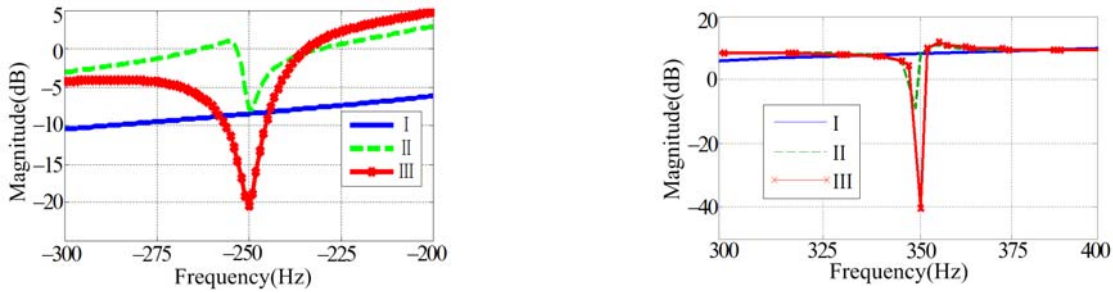

Fig. 7. Magnitude-frequency characteristic curves of the output impedance with the three control strategies, (a) with 5th negative-sequence harmonic compensation, (b) with 7th positive-sequence harmonic compensation.

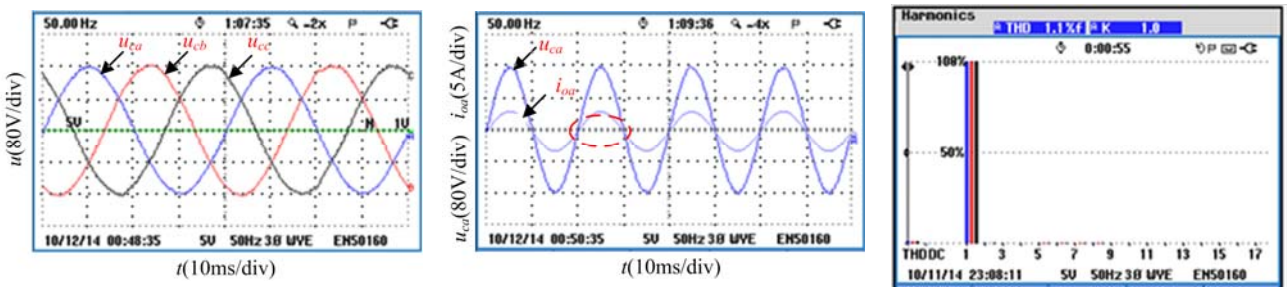

Fig. 8. Experimental waveforms with an RL linear load using the conventional control strategy, (a) three-phase voltage waveforms, (b) A-phase voltage and current waveforms, (c) line voltage harmonics spectrum.

frequencies. The output impedance shown in Fig.7 matches well with the above theoretical analysis, which demonstrates that the feedforward control strategy with the PNSHR is highly effective, i.e., the output impedance is attenuated effectively at specific frequencies. Therefore, the proposed load current feedforward compensation scheme can effectively suppress load harmonics.

V. Experimental Results

A 5kVA PV off-grid inverter has been built to verify the proposed strategy. The power circuit is shown in Fig.1. The control algorithm is implemented in a DSP TMS320F28335, a Xilinx XC3S400 FPGA is used to realize the circuit design function based on hardware description language, and experimental waveforms are measured by a FLUKE 435. The experimental parameters are shown in Table I.

First, Fig. 8 shows experimental results with linear RL loads using the conventional control strategy. Fig. 8(a) shows three-phase output voltage waveforms of an off-grid inverter. A-phase output voltage and current waveforms are shown in Fig. 8(b). The harmonics spectrum of the output line voltage is shown in Fig. 8(c) which is 1.1%. With these results, a good control performance is verified under linear loads.

Then, a diode rectifier is used as a nonlinear load. Fig. 9(a) shows output voltage waveforms of an off-grid inverter. Voltage and current waveforms of nonlinear loads are shown in Fig. 9(b). The harmonics spectrum of the line voltage is shown in Fig. 9(c). The harmonics injected into the output voltage of the inverter include the 5th, 7th, 11th and 13th harmonics, where the 5th and 11th are the negative sequence harmonics, the 7th and 13th are the positive sequence harmonics. However, the 5th and 7th harmonics are higher. As can be seen, the output voltage with a THD of 6.0% is heavily distorted by the load harmonic current.

To evaluate the proposed feedforward compensation strategy and to verify its effectiveness, experiments were performed using three feedforward methods for comparison: the unity feedforward control strategy, the feedforward control strategy using a PNSHR without parameters revision, and the feedforward control strategy using PNSHR parameters revision. The three-phase voltages, the line voltage harmonics spectrum, and the A-phase voltage and current waveforms, are shown in Fig. 10, Fig. 11 and Fig. 12.

Fig. 10 shows experimental waveforms under the unity feedforward control strategy of the load current with a nonlinear load. Fig. 11 shows experimental waveforms under the unrevised PNSHR feedforward control strategy. The 5th and 7th harmonics of the output voltage shown in Fig. 10(b) are 4.2%. They are 2.1% in Fig. 10(c), 4.1% in Fig. 11(b) and 2.2% in Fig. 11(c). It can be seen that the 5th and 7th harmonics of the first two strategies are similar, which matches well with the theoretical analysis. The feedforward control strategy using a PNSHR without parameters revision

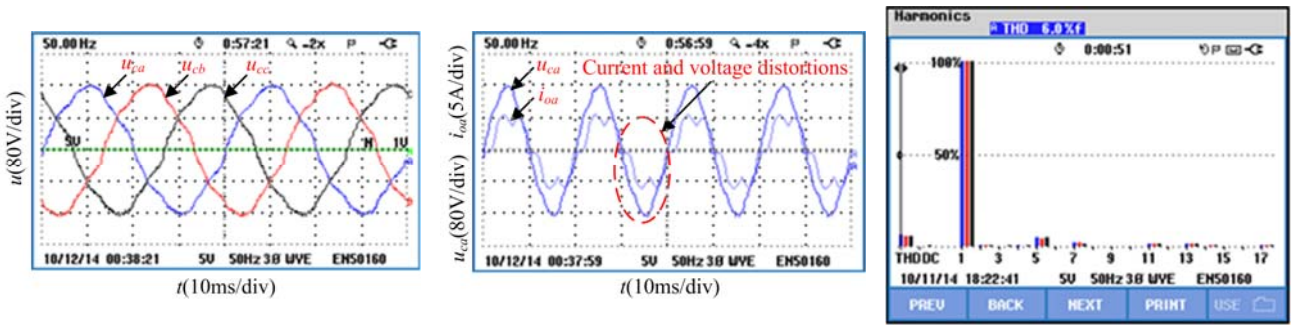

(a) (b) (c)

Fig. 9. Experimental waveforms with a nonlinear load, (a) three-phase voltage waveforms, (b) A-phase voltage and current waveforms, (c) line voltage harmonics spectrum.

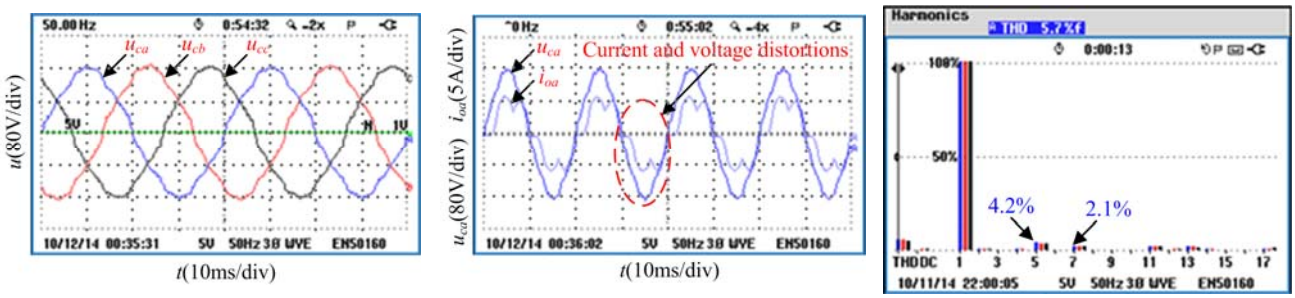

(a) (b) (c)

Fig. 10. Experimental waveforms under the unity feedforward control strategy of a load current with a nonlinear load, (a) three-phase voltage waveforms, (b) A-phase voltage and current waveforms, (c) line voltage harmonic spectrum.

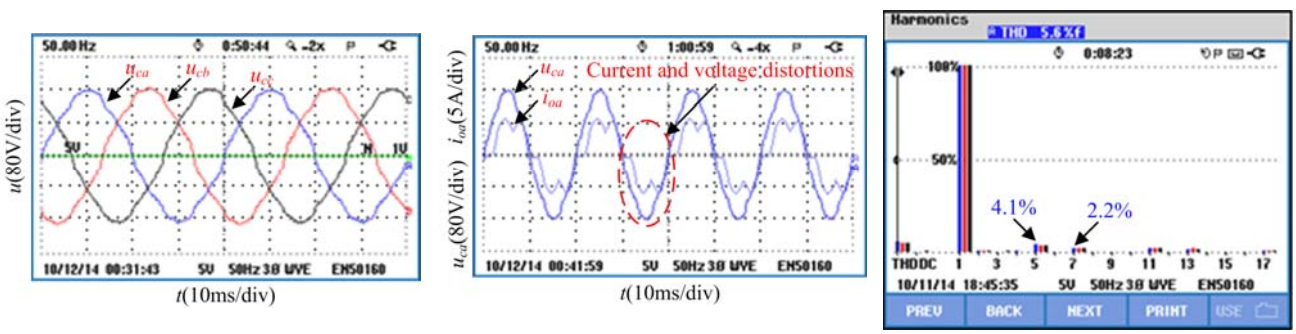

(a) (b) (c)

Fig. 11. Experimental waveforms under the unrevised PNSHR feedforward control strategy, (a) three-phase voltage waveforms, (b) A-phase voltage and current waveforms, (c) line voltage harmonic spectrums.

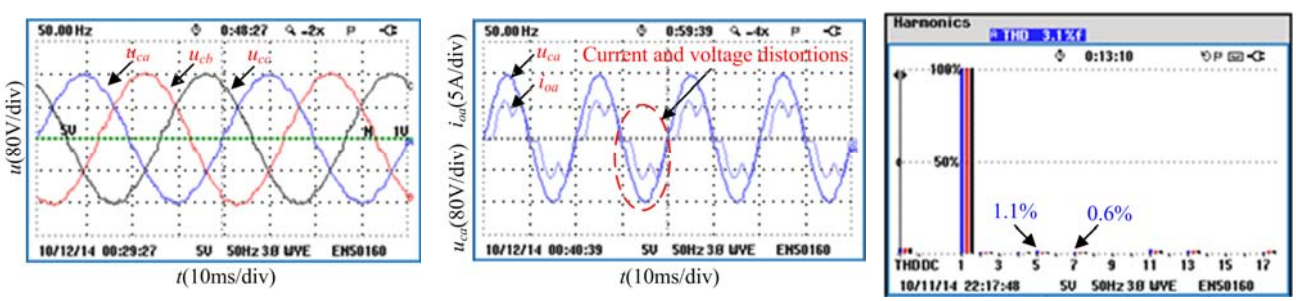

(a) (b) (c)

Fig. 12. Experimental waveforms under the revised PNSHR feedforward control strategy, (a) three-phase voltage waveforms, (b) A-phase voltage and current waveforms, (c) line voltage harmonics spectrum.

cannot fully suppress the harmonics. The 5th and 7th harmonics of the output voltage with the feedforward control strategy using PNSHR parameter revision are 1.1% and 0.6%, and the total harmonic distortion rate is 3.1%, as shown in Fig. 12(c). The experimental results show that the proposed method can compensate load harmonics effectively, i.e., it has a good ability to suppress the effects of load current harmonics on the output voltage.

VI. Conclusions

Suppression of the output-voltage harmonics for off-grid inverters based on the output impedance has been investigated in this paper. Based on the conventional droop control, a dual-closed-loop control strategy with inductor current and filtering-capacitor voltage feedback is adopted. To improve the performance of off-grid inverters and to damp the LC filter resonant, an extra load current feedforward loop has been added in the control scheme. An improved feedforward compensation strategy has been proposed based on the PNSHR and the parameters are then revised to minimize the output voltage harmonics caused by nonlinear loads. The experimental results match well with the analysis. They show that with the proposed strategy, the output impedance is effectively suppressed with reduced output voltage harmonics at selective harmonic frequencies.

Appendix

Combining (14) and (19), $W(j\omega_h)$ can be expressed as:

$$W(j\omega_h) = G_P(j\omega_h) = \frac{A_h\omega_c}{j\omega_h - j\omega_{0h} + \omega_c} = \frac{A_h}{j\dfrac{\omega_h - \omega_{0h}}{\omega_c} + 1} \tag{A1}$$

$$\| W(j\omega_h) \| = A_h \frac{\sqrt{1+x^2}}{1+x^2} = \frac{A_h}{\sqrt{1+x^2}} \tag{A2}$$

$$\tan \angle W(j\omega_h) = -x \tag{A3}$$

where, $x = \dfrac{\omega_h - \omega_{0h}}{\omega_c}$. In addition, x can be expressed as A.4 according to (20).

$$x = \tan \angle F(j\omega_h) \tag{A4}$$

Therefore, (21) can be obtained from (A2), (A3) and (A4). In addition, (22) can be obtained in a similar manner.

References

[1] J. G. de Matos, F. S. F. e Silva, and L. A. de S. Ribeiro, "Power control in AC isolated microgrids with renewable energy sources and energy storage systems," *IEEE Trans. Ind. Electron*., Vol. 62, No. 6, pp. 3490-3498, Jun. 2015.

[2] T. Jin and J. A. Jimenez, "A review on planning and automation technologies for distributed generation systems," in *IEEE Conference on Automation Science and Engineering (CASE)*, pp. 269-274, Aug. 2010.

[3] K. S. Herman, "Attracting foreign direct investment the Chilean government's role promoting renewable energy," in *International Conference on Renewable Energy and Applications (ICRERA)*, pp.37-41, Oct. 2013.

[4] J. M. Guerrero, L. Hang, and J. Uceda, "Control of distributed uninterruptible power supply systems," *IEEE Trans. Ind. Electron*., Vol. 55, No. 8, pp. 2845-2859, Aug. 2008.

[5] J. C. Vasquez, J. M. Guerrero, M. Savaghebi, J. Eloy-Garcia, and R. Teodorescu, "Modeling, analysis, and design of stationary reference frame droop controlled parallel three-phase voltage source inverters," *IEEE Trans. Ind. Electron.*, Vol. 60, No. 4, pp. 1271-1280, Apr. 2013.

[6] A. A. Ghadimi, F. Razavi, and R. Ghaffarpour, "Control of islanded inverter interfaced distributed generation units for power quality improvement," in *14th International Conference on Harmonics and Quality of Power (ICHQP)*, pp. 1-6, Sep. 2010.

[7] J. Rocabert, A. Luna, F. Blaabjerg, and P. Rodriguez, "Control of power converters in AC microgrids," *IEEE Trans. Power Electron.*, Vol. 27, No. 11, pp. 4734-4749, Nov. 2012.

[8] Y. W. Li, "Control and resonance damping of voltage-source and current-source converters with LC filters," *IEEE Trans. Ind. Electron.*, Vol. 56, No. 5, pp. 1511-1521, May 2009.

[9] R. Majumder, A. Ghosh, G. Ledwich, and F. Zare, "Power sharing and stability enhancement of an autonomous microgrid with inertial and non-inertial DGs with DSTATCOM," in *International Conference on Power Systems (ICPS)*, pp. 1-6, Dec. 2009.

[10] A. Lidozzi, L. Solero, S. Bifaretti, and F. Crescimbini, "Sinusoidal voltage shaping of inverter-equipped stand-alone generating units," *IEEE Trans. Ind. Electron*., Vol. 62, No. 6, pp. 3557 - 3568, Jun. 2015.

[11] A. Singh, M. Badoni, and B. Singh, "Power sharing in distributed power generation system," in *IEEE 5th India International Conference on Power Electronics (IICPE),* pp. 1-6, Dec. 2012.

[12] R. B. Gonzatti, S. C. Ferreira, C. H. da Silva, L. E. B. da Silva, G. Lambert-Torres, and L. G. F. Silva, "Hybrid active power filter applied to harmonic compensation of current-source type and voltage-source type nonlinear loads," in *Brazilian Power Electronics Conference (COBEP)*, pp. 1257-1262, Oct. 2013.

[13] S. Ratanapanachote, M. Kang, and P. N. Enjeti, "Auto-connected electronic phase-shifting transformer concept for reducing harmonic generated by nonlinear loads in electric power distribution system," in *IEEE 32nd Annual Power Electronics Specailists Conference (PESC)*, Vol. 2, pp. 1030-1035, Jun. 2001.

[14] R. Ortega, C. L. Trujillo, G. Garcera, E. Figueres, and O. Carranza, "A PI-P+Resonant controller design for single phase inverter operating in isolated microgrids" in *IEEE International Symposium on Industrial Electronics (ISIE)*, pp. 1-6, May 2012.

[15] W. Li, D. Pan, X. Ruan, and X. Wang, "A full-feedforward scheme of grid voltages for a three-phase grid-connected inverter with an LCL filter," in *IEEE Energy Conversion Congress and Exposition (ECCE)*, pp. 96-103, Sep. 2011.

[16] X. Wang, X. Ruan, S. Liu, and C. K. Tse, "Full

feedforward of grid voltage for grid-connected inverter with LCL filter to suppress current distortion due to grid voltage harmonics," *IEEE Trans. Power Electron.*, Vol. 25, No. 12, pp .3119-3127, Dec. 2010.
[17] Y. Qi, L. Peng, M. Chen, and Z. Huang, "Load disturbance suppression for voltage-controlled three-phase voltage source inverter with transformer," *IET Power Electronics*, Vol. 7, No. 12, pp. 3147-3158, Dec. 2014.
[18] T. Ye, N. Y. Dai, C. S. Lam, M. C. Wong, and J. M. Guerrero, "Analysis, design and implementation of a quasi-proportional-resonant controller for multifunctional capacitive-coupling grid-connected inverter," *IEEE Trans. Ind. Appl.*, Vol. 52, No. 5, pp. 4269-4280, Sep./Oct. 2016.
[19] F. de Bosio, L. A. de S. Ribeiro, F. D. Freijedo, M. Pastorelli, and J. M. Guerrero, "Effect of state feedback coupling and system delays on the transient performance of stand-alone VSI with LC output filter," *IEEE Trans. Ind. Electron.*, Vol. 63, No. 8, pp, 4909-4918, Apr. 2016.
[20] S. Guo and D. Liu, "Analysis and design of output LC filter system for dynamic voltage restorer," *in 26th Annual IEEE Applied Power Electronics Conference and Exposition (APEC)*, pp. 1599-1605, Mar. 2011.
[21] K. Hatua, A. K. Jain, D. Banerjee, and V. T. Ranganathan, "Active damping of output LC filter resonance for vector-controlled VSI-fed AC motor drives," *IEEE Trans. Ind. Electron*., Vol. 59, No. 1, pp. 334-342, Jan. 2012.
[22] E. Figueres, G. Garcera, J. Sandia, F. Gonzalez-Espin, and J. C. Rubio, "Sensitivity study of the dynamics of three-phase photovoltaic inverters with an LCL grid filter," *IEEE Trans. Ind. Electron*., Vol. 56, No. 3, pp. 706-717, Mar. 2009.
[23] X. Wu, X. Li, X. Yuan, and Y. Geng, "Grid harmonics suppression scheme for LCL-type grid-connected inverters based on output admittance revision," *IEEE Trans. Sustain Energy*., Vol. 6, No. 2, pp. 411-421, Apr. 2015.
[24] J. L. Agorreta, M. Borrega, J. Lopez, and L. Marroyo, "Modeling and control of N-paralleled grid-connected inverters with LCL filter coupled due to grid impedance in PV plants," *IEEE Trans. Power Electron.*, Vol. 26, No. 3, pp. 770-785, Mar. 2011.
[25] L. Cao, K. H. Loo, and Y. M. Lai, "Systematic derivation of a family of output-impedance shaping methods for power converters-A case study using fuel cell-battery-powered single-phase inverter system," *IEEE Trans. Power Electron*., Vol. 30, No. 10, pp. 5854-5869, Oct. 2015.
[26] P. Cortes, D. O. Boillat, H. Ertl, and J. W. Kolar, "Comparative evaluation of multi-Loop control schemes for a high-bandwidth AC power source with a two-stage LC output filter," in *International Conference on Renewable Energy Research and Applications* (*ICRERA*), pp. 1-10, Nov. 2012.
[27] Y. Qi, L. Peng, M. Chen, and Z. Huang, "Load disturbance suppression for voltage-controlled three-phase voltage source inverter with transformer," *IET Power Electronics*, Vol. 7, No. 12, pp. 3147-3158, Dec. 2014.

Yiwen Geng was born in Jiangsu Province, China, in 1977. He received his B.S., M.S. and Ph.D. degrees in Electric Engineering from the School of Information and Electrical Engineering, China University of Mining and Technology, Xuzhou, China, in 2000, 2004 and 2014, respectively. From 2006 to 2016, he was a Lecturer in the School of Information and Electrical Engineering, China University of Mining and Technology. Since 2016, he has been with the Department of Electrical and Power Engineering, China University of Mining and Technology, where he is presently working as an Associate Professor. His current research interests include photovoltaic inverters, harmonic mitigation and power electronics.

Xue Zhang was born in Anhui Province, China, in 1988. She received her B.S. and M.S. degrees in Electrical Engineering from the China University of Mining and Technology, Xuzhou, China, in 2013 and 2016, respectively. She is presently working in the Patent Examination Cooperation Center of the Tianjin Patent Office SIPO. Her current research interests include power electronics, renewable energy generation systems and microgrids.

Xiaoqiang Li received his B.S. and Ph.D. degrees from the School of Information and Electrical Engineering, China University of Mining and Technology, Xuzhou, China, in 2010 and 2015, respectively. He is presently a Research Fellow in the School of Electrical and Electronic Engineering, Nanyang Technological University, Singapore. His current research interests include renewable energy generation and digital control in power electronics.

Kai Wang was born in Anhui, China, in 1992. He received his B.S. degree in Electrical Engineering and Automation, and his M.S. degree in Electrical Engineering from the China University of Mining and Technology, Xuzhou, China, in 2013 and 2016, respectively, where he is presently working toward his Ph.D. degree in Electrical Engineering. His current research interests include the control of PWM converters, parallel converter systems and photovoltaic generation technologies.

Xibo Yuan (S'09–M'11) received his B.S. degree from the China University of Mining and Technology, Xuzhou, China, in 2005; and his Ph.D. degree from Tsinghua University, Beijing, China, in 2010, both in Electrical Engineering. Since 2016, he has been a Reader in the Electrical Energy Management Group, Department of Electrical and Electronic Engineering, University of Bristol, Bristol, ENG, UK, where he became a Lecturer and a Senior Lectuer, in 2011 and 2015, respectively. He was a Visiting Scholar at the Center for Power Electronics Systems, Virginia Polytechnic Institute and State University, Blacksbug, VA, USA, and at the Institute of Energy Technology, Aalborg University, Aalborg, Denmark. He was a Postdoctoral Research Associate in the Electrical Machines and Drives Research Group, Department of Electronic and Electrical Engineering, University of Sheffield, Sheffield, ENG, UK. His current research interests include power electronics and motor drives, wind power generation, multilevel converters, the application of wide-bandgap devices, and more electric aircraft technologies.